J Mater Sci (2006) 41:6396–6402
DOI 10.1007/s10853-006-0717-0

Electrical properties of EVA filled by zinc powder

**J. R. Subiela · J. López · R. Balart ·
J. J. García-Jareño · F. Vicente**

Received: 21 July 2004 / Accepted: 13 July / Published online: 29 August 2006

Abstract Elastic composites of zinc powder directly dispersed within an EVA (ethylene-vinyl acetate) matrix were prepared by a hot plates procedure. Conductance of samples depends on the filler content in three different regimes: polarization, tunnelling effect and percolation. The surface corrosion was monitored by means of optical, SEM and EDX methods, and after that the loss of mass was checked. The corrosion only affects to the zinc particles placed of the surface of the composite samples.

Introduction

Physical properties of composite materials have been widely studied due to their industrial applications [1–3]. Among the composite materials, those which consist of an isolator phase (generally a polymer) filled with metal or another conductive powder (graphite, aluminium, zinc...) are of special interest in electrochemistry. Those materials combine the isolator properties of the polymer phase with conductive behaviour of the filler. They represent a very important group in the engineering science with a large range of applications, like corrosion prevention, shielding and electromagnetic interferences absorption, electrostatic unload, heat conduction, mechanical to electrical signal conversion, rechargeable batteries, etc [4–7].

The electrical properties of the composite materials are strongly dependent on their surface characteristics. The percolation theory states that electrical conduction depends on the volume fraction of the conductive phase in the bulk of the material. Particles in the composite were disposed forming clusters, some of them cross the whole of the material from one side to the other forming the backbone cluster or percolation cluster, through which the electrical conduction takes place [8, 9]. But to form these conductive paths a metal volume fraction threshold must be surpassed, named ‘first percolation threshold’ v_c, which varies from one material to another as a function of components densities and packing system [10–16]. Generally, it is possible to calculate the volume fraction threshold by means of its electrical properties, relating the resistance with the volume fraction v of the conductive material [17, 18]. For a percolative process with two phases in three dimensions, the sum of the percolation threshold probabilities is equal to the unity, $pc_1 + pc_2 = 1$. The relation between the volume fraction (v) and the percolation probability is $v = f \cdot \mathrm{p}$, where f is the packing factor, which has different values for each packing system, e.g. $f = \pi/6$, for a cubic regular simple distribution, and $f = (\sqrt{3/8})\pi$ for a cubic centred simple [19].

Another characteristic for this kind of materials is the fact that the presence of metallic particles in the surface makes these materials susceptible to corrosion processes, so the study of this phenomenon is of interest [20, 21].

J. R. Subiela · J. J. García-Jareño · F. Vicente (✉)
Department of Physical Chemistry, University of Valencia,
C/ Dr. Moliner 50, E-46100 Burjassot, Valencia, Spain
e-mail: Francisco.Vicente@uv.es

J. López · R. Balart
Department of Mechanical Ingeniery and Materials,
Politecnic University of Valencia, EPSA, Avda Viaducte, 1,
E-03801 AlicanteAlcoi, Spain

Previous studies about polymer matrix composites filled with zinc powder were done [22–25], but no one about this elastic material. The EVA copolymer (ethylene-vinyl acetate) was filled with increasing amounts of powder zinc, from 10 to 75 wt%. Both materials are of technological usefulness: zinc proves very important on preventing corrosion systems and batteries, whereas EVA is an elastic polymeric material with a low melting point. Then, the properties of the mixtures of both materials or ‘‘product properties’’ are of promising usefulness. The aim of this work is to characterize the electrical properties of the composite made with a different ratio of powder zinc dispersed within the polymeric matrix. Also, studies on the effect of an aqueous acid/basic attack as corrosion simulation at the laboratory were done. Besides, some other physical properties were related with the observed electrical behaviour.

Experimental

Composite preparation

Plates (120 × 60 × 4 mm) of polymeric matrix composites filled with metal powder were obtained by directly mixing grains of EVA copolymer (20% vinyl acetate) (REPSOL Química, S.A., Puertollano, Spain) previously pulverized, with different amounts of powder zinc (MERCK) (10, 20, 30, 40, 50, 60, 62.5, 65, 70, 72.5 and 75 Zn wt%). The mixture was later on put in hot plates with a constant 10 kg cm^{-2} pressure for 180 s at 393 K, followed with chilling to 313 K for 600 s. The zinc mass fraction can be related with the zinc volume fraction by

$$v_{\mathrm{Zn}} = \frac{\frac{m_{\mathrm{Zn}}}{\rho_{\mathrm{Zn}}}}{\frac{m_{\mathrm{Zn}}}{\rho_{\mathrm{Zn}}} + \frac{(1-m_{\mathrm{Zn}})}{\rho_{\mathrm{EVA}}}} \tag{1}$$

where v_{Zn} and m_{Zn} are volume and mass fraction of zinc in the sample, and ρ_{Zn} and ρ_{EVA} are Zn and EVA densities (7.14 and 0.91 g cm^{-3}, respectively) [26].

Optical characterization

Images of composite surfaces were acquired with a commercial scanner (Genius ColorPage-HR6X) connected to a PC. Both brightness and contrast were always adjusted at the same values. From the scanned images, colour histograms were obtained by using the capabilities of *The Gimp 2.0* software [27]. Average values given by these colour histograms were used in this study.

Microanalysis (EDX) and SEM

A Phillips XL30 ESEM was used. Samples were fixed on an aluminium shelf. Work conditions were: E = 20 kV, t_{live} = 120 s. *w.d.* = 10.000 mm (potential, live time and working distance, respectively). The two sides of the samples were separately observed in order to study the effect of gravity on the zinc dispersion during the composite preparation.

Electrical properties

Samples of 83 × 53 × 3.5 mm were used for these measurements. Two nickel electrodes 15 × 60 mm. were disposed in parallel and symmetrically on each side of the composite and connected to a Phillips PM 6304 ‘Programmable Automatic RCL Metter’ (RCL Metter) by means of cupper wires, where the distance between the two electrodes was the thickness of the samples (3.5 mm.). Values of R, C, $|Z|$ and Φ (resistance, capacitance, impedance modulus and phase angle, respectively) were obtained at E = 0 V and E = 2 V and with different amplitudes: $\Delta E_{\mathrm{Low}} = \pm 50$ mV, $\Delta E_{\mathrm{Normal}} = \pm 1$ mV and $\Delta E^{\mathrm{High}} = \pm 2$ V, always at frequency of 100 kHz, where E is the applied potential and ΔE the superimposed potential.

Corrosion simulation: acid–base treatment

Samples of 40 × 10 × 3.5 mm were cut and put in HDPE containers with 100 mL of solution 0.5 M KCl (SIGMA a.c.s reagent), pH = 4.5 acidulated with HCl (PROLABO analytical reagent. The acid treatment was:

(1) One week in acidulated water with HCl (pH = 4.5) at room temperature, stirring in an ultrasounds bath at 50 °C for 30 min each day.
(2) One day in an acid solution by carrying the solutions to pH = 1.5 by HCl addition and afterwards stirred for 30 min in an ultrasounds bath at 50 °C.
(3) 26 days in a basic solution by carrying the solutions to pH = 9 by KOH addition.

After the treatment, the samples were rinsed with 20 mL of HAc/Ac$^-$ 1 M buffer solution (HAc and KAc supplied by Scharlau a.c.s reagent), and dried at room temperature.

The mass of samples was measured for three times before and after the acid treatment. The 20 mL of HAc/Ac$^-$ buffer solutions used in the rising of each sample, were added to the solutions where samples came from.

Differential pulse anodic stripping voltammetry (DPASV) of the bath solutions

After rinsing with HAc/Ac^- buffer, 5 mL of resultant solutions + 5 mL HAc/Ac^- 1 M buffer solution + 10 mL KCl 0.5 M (to adjust cell volume), were analysed by DPASV in order to determine the amount of zinc dissolved [28–29]. The reference electrode was a $Ag/AgCl/KCl_{sat}$ electrode, the counter electrode was a Pt bar, and a 3.65 mm. diameter circular graphite, previously polished, sunk in HCl and cycled for three times in water, was the working electrode. The solution was deaerated for 5 min with Ar (Air Liquide) before starting each experiment. Experimental conditions were: cathodic deposition $t_{dep} = 180$ s, potential applied $E_{dep} = -1.4$ V, stabilisation time $t_{rest} = 30$ s. Voltammograms where made between $E^i = -1.2$ V and $E^f = -0.8$ V, applying pulses of 20 mV with steeps of $\Delta E = 4$ mV, and recorded at a scan rate of $v = 10$ mv s^{-1}. After each experiment a 0.2 V potential was applied for 120 s in order to clean the working electrode surface. A calibration curve (10^{-4}–10^{-6} M) was obtained with $ZnCl_2$ (MERCK p.a.). All solutions were prepared with distilled and deionised (Mili Q-plus MILIPORE) water.

Electrical properties of the corroded samples

To carry out these experiments, the acid treatment was repeated with new composite tablets of 85 × 43 × 3.5 mm size, but with the following modifications:

(1) Seven hours in acidulated water with HCl (pH = 4.5) at room temperature, stirring in an ultrasounds bath at 50 °C for 30 min each hour.
(2) One hour in an acid solution by carrying the solutions to pH = 1.5 by HCl addition, and afterwards stirred for 30 min in an ultrasounds bath at 50 °C within the same solution.
(3) One hour in a basic solution by carrying the solutions to pH = 9 by KOH addition.

After that, samples were rinsed with 20 mL HAc/Ac^- 1 M buffer solution. Nevertheless, the experimental data acquisition method was the same as it was in the non-treated samples.

Results and discussion

Optical characterization

Images of the surface samples were acquired with a commercial scanner. In spite of the fact that it could seem to be a non-rigorous methodology, it presents some advantages if compared with other ways of acquiring images. The most important difference is the fact that the artefacts caused by the shadows on the image, introduced by a particular light incidence, are drastically reduced and the images can be easily analysed by different software packages. A good parameter which allows the comparison between different samples is the analysis of the colour histogram for different samples, and in particular, the average value (Fig. 1). The histogram includes the brightness values of the pixels of an image in a scale which ranges from 0 (dark) to 255 (clear). The mean of the histogram shows the average distribution of the brightness of the pixels. This mean value increases with the zinc mass fraction up to samples of 60 wt% in Zn. This seems to indicate that there is a saturation of zinc presence in the composite surface over this ratio in zinc. On the other hand, it is necessary to remark the high reproducibility of the obtained values.

Microanalysis (EDX)

Microanalysis by mean EDX confirms the results obtained from the optical characterization where the zinc surface saturation takes place at about 50 wt% in zinc. The difference between the 60 wt% and 50 wt% for zinc surface saturation derived from

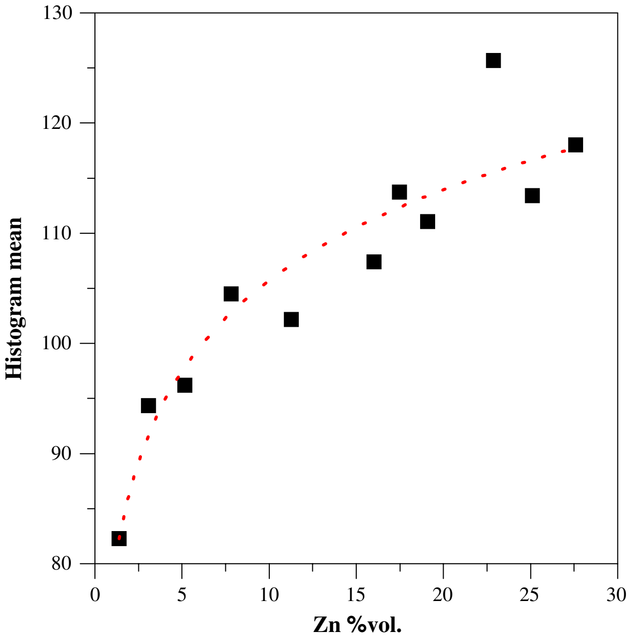

Fig. 1 Mean values of the colour histogram of the images obtained with *The Gimp 2.0* software from images acquired with Genius ColorPage-HR6X scanner connected to a PC

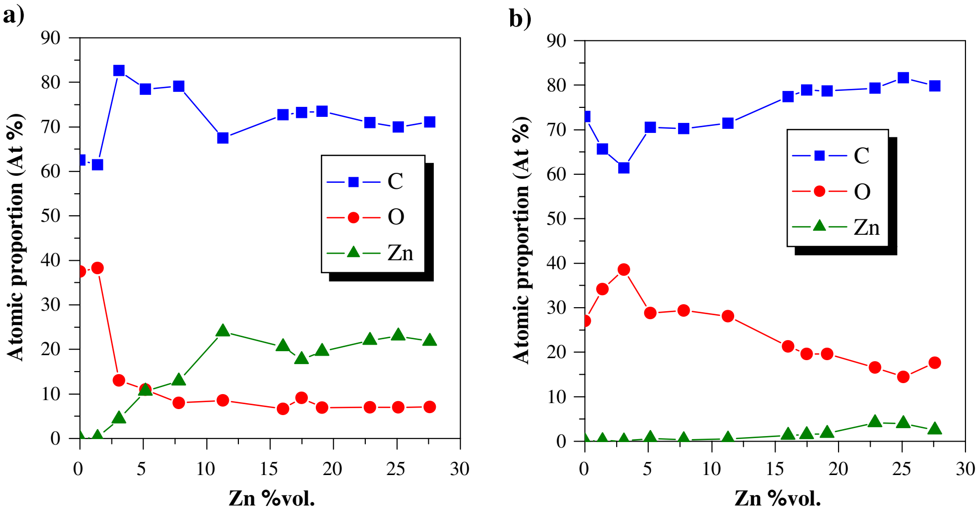

Fig. 2 EDX results for all samples (Zn, C and O At%) before (**a**) and after (**b**) acid treatment. Phillips XL30 ESEM. E = 20 kV, t_{live} = 120 s, *w.d.* = 10.000 mm

these two techniques was assumed to be caused by the different depth penetration of each technique into the composite structure: by means of the scanner method only the outer surface is observed, whilst EDX penetrates a few micrometers. Figure 2 shows EDX the normalized number of accounts At% results for all samples. The oxygen presence decreases with Zn increases and C keeps practically constant. Oxygen atoms come from acetate groups of the polymeric phase, and they are orientated to the exterior of the bulk by electrostatic forces in the composite formation at low zinc concentrations. But if the zinc mass fraction increases, these acetate groups envelope the metal atoms forming conglomerates of zinc which are coordinated with the acetates, where the electron delocalisation and interactions between the zinc and the polymer were favoured. These polymer–zinc interactions force cluster formation in certain directions and the zinc surface presence was limited by this phenomenon. Little differences between the two sides (upper and lower) of composites were observed. This is due to the gravity effect in composite preparation, magnified by the high density of zinc.

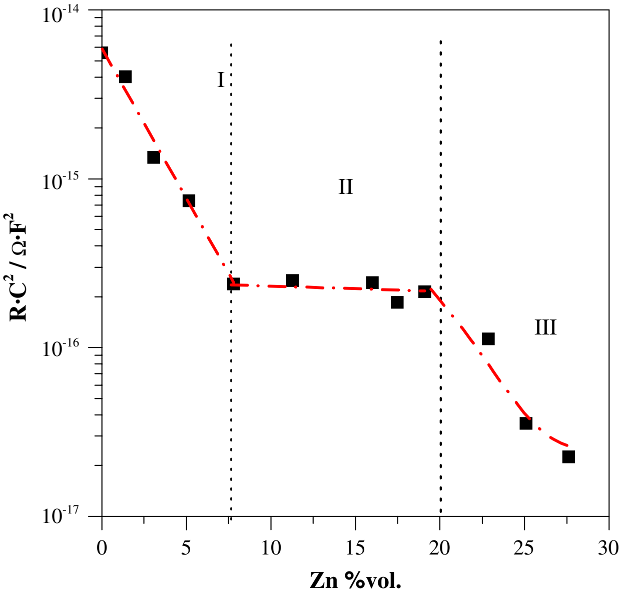

Fig. 3 $R{\bullet}C^2$ values calculated from data obtained with Phillips PM 6304 RCL Metter. An $E = 2$ V potential and an ac superposed current of potential amplitude $\Delta E = \pm 2$ V was applied, at a frequency of 100 kHz. A = 9 cm^2, T = 25 °C. It is possible to distinguish three intervals: zone I related with clusters formation and isolator behaviour; zone II related to cluster growth and tunnelling conduction; and zone III related to backbone cluster formation and conduction by percolation

Electrical properties

The dielectric constant and the conductivity obtained at high frequency evolve in consonance with the zinc amount present in the polymeric matrix (Table 1). Figure 3 shows the $R{\cdot}C^2$ product dependence on the zinc amount in the samples. There are three well defined zones. In the first one, zone I, the $R{\cdot}C^2$ product decreases linearly. In this zone, the initial zinc clusters are forming, surely orientated by the polymer phase, especially by the acetate groups. High isolator behaviour can be observed in this zone and the electrical perturbation causes a polarization phenomenon. The phase angle Φ remains close to $\pi/2$ rad. as corresponds to a capacitive behaviour without electrical conductance (Table 1). Zone II is a stable zone for the

Table 1 Electrical properties of the EVA-Zn composites. Philips PM 6304 RCL Metter. $E = 2$ V, $\Delta E = \pm 2$ V, $f = 100$ kHz. $A = 9$ cm^2, $T = 25$ °C

Zn wt$_i$. (%)	Zn v_i (%)	R (kΩ)	C (pF)	Ω (°)	|Z| (kΩ)	ρ (kΩ cm)	ϵ (pF cm^{-1})
0	0	46,400	11	–90	149	1.19×10^6	0.43
10	1.4	31,600	11	–90	143	8.11×10^5	0.44
20	3.1	5,050	16	–89	103	1.30×10^5	0.63
30	5.2	2,370	18	–87	92.6	6.10×10^4	0.69
40	7.8	733	18.0	–83	87.7	1.88×10^4	0.70
50	11.3	454	24	–82	67.0	1.17×10^4	0.91
60	16.0	194	35	–77	43.9	4.99×10^3	1.4
62.5	17.5	132	38	–72	40.6	3.41×10^3	1.5
65	19.1	106	45	–71	33.5	2.72×10^3	1.7
70	22.9	18.9	77	–38	13.6	487	3.0
72.5	25.1	6.70	73	–17	6.30	172	2.8
75	27.6	1.20	140	–6	1.20	31.7	5.3

electrical properties of the bulk, where the product $R{\cdot}C^2$ remains constant, since the changes of the time constant $R{\cdot}C$ are not as big as the variations in the other zones. A low conductivity of the solid was obtained in this zone, which can be attributed to a tunnelling conduction [30–32], where the terminal parts of zinc clusters act as microelectrodes and the polymeric phase between two close neighbour clusters acts as a high potential barrier zone. That way, these microelectrodes separated by a dielectric phase must also act as capacitors; therefore the system resultant capacitance must increase with the zinc volume fraction at the same time as the resistance diminishes, since it is possible to form clusters of zinc particles separated by less than 10^{-8} m. Finally, zone III shows a decrease on the $R{\cdot}C^2$ curve due to an important resistance decrease which can overcome the capacitance increase. This is the initial part of the percolative conduction. In this zone, an infinite percolation cluster has just formed and electric conductivity begins trough the backbone cluster.

Taking into account the results of previous studies on HDPE + graphite powder composites [17], if the zinc and graphite densities are considered (7.14 and 2.25 g cm^{-3}, respectively [26]) and provided that EVA and HDPE have similar densities, it is possible to approximately calculate a theoretical volume fraction threshold for the EVA + Zn composites through the approximate equation:

$$v_c^{\mathrm{Zn}} = v_c^{\mathrm{C}} \cdot \frac{\rho_{\mathrm{Zn}}}{\rho_{\mathrm{C}}} \tag{2}$$

where v_c^{Zn} and v_c^{C} are the percolation volume fraction for zinc and graphite, and ρ_{Zn} and ρ_{C} their correspondent densities. That way, a theoretical threshold $v_{t,c}^{\mathrm{Zn}} = 0.44$ (83 wt%) was calculated. However, from the dependence of the resistance on the volume fraction of zinc (Table 1), a lower value of $v_c^{\mathrm{Zn}} = 0.195 \pm 0.05$ was obtained, that is, the percolation phenomenon appears at lower values of v than it was expected. This is due to the formation of aggregates of zinc particles, which favours the cluster growth, therefore decreasing the metal filler volume fraction threshold at which the backbone cluster appears. Also it is necessary to consider that the percolation threshold depends on the size and shape of the metal filler as well as on the procedure used for preparing the samples [33–35].

Characterization of the samples after the acid treatment

Table 2 shows a comparison between the zinc mass loss calculated from differential pulse stripping analysis (DPASV) experiments and the composite mass loss obtained from the sample weighting before and after

Table 2 Comparison between zinc mass loss calculated from DPASV study ($\Delta m_i^{\mathbf{Zn}}$) and composite mass loss calculated from sample weighting before (m_i) and after chemical treatment ($\Delta m_i^{\mathbf{EVA\text{-}Zn}}$). Also shown the relative mass loss (%Δm_i) as

Sample (Zn wt%)	m_i (g)	Δm_i^{Zn} (mg)	$\Delta m_i^{\mathrm{EVA\text{-}Zn}}$ (mg)	%Δm_i (%)
0	1.6096	0.068	0.367	0.02
10	1.6097	3.964	4.500	0.28
20	1.4821	7.366	7.800	0.53
30	1.8904	15.198	15.367	0.81
40	2.3175	16.033	29.167	1.26
50	2.1077	15.906	32.567	1.55
60	2.4030	17.121	34.600	1.44
62.5	2.8369	17.009	37.733	1.33
65	2.4773	17.855	35.567	1.44
70	3.3452	17.310	53.500	1.60
72.5	3.4824	17.405	50.167	1.44
75	3.4737	17.136	51.567	1.48

Table 3 Electrical properties of the EVA-Zn composites after acid attack. Philips PM 6304 RCL Metter. An E = 2 V potential and an ac superposed current of potential amplitude $\Delta E = \pm 2$ V was applied, at a frequency of 100 kHz. A = 9 cm^2, T = 25 °C

Zn wt$_i$. (%)	Zn v_i (%)	R (kΩ)	C (pF)	Φ (°)	$\|Z\|$ (kΩ)	ρ (kΩ cm)	ϵ (pF cm^{-1})
0	0	24,900	8.9	–90	179	6.40×10^5	0.35
10	1.4	17,700	11	–90	142	4.55×10^5	0.44
20	3.1	5,640	12	–89	133	1.45×10^5	0.46
30	5.2	2,130	14	–87	111	5.47×10^4	0.56
40	7.8	353	20	–78	76.2	9.08×10^3	0.79
50	11.3	229	33	–78	46.7	5.88×10^3	1.3
60	16.0	43.1	54	–56	24.2	1.11×10^3	2.1
62.5	17.5	61.4	51	–63	28.0	1.58×10^3	2.0
65	19.1	2.81	120	–12	2.76	72.3	4.5
70	22.9	3.10	11	–17	2.97	79.7	4.5
72.5	25.1	16.2	110	–50	10.6	417	4.4
75	27.6	0.525	250	–5	0.523	13.5	9.6

acid treatment. It is easy to see that not all composite mass loss corresponds to zinc loss. That means that not only zinc passes to the solution, but also that the polymer phase does. Probably acetate groups that were enveloping zinc particles had accompanied those forming coordinating complexes. That agrees with the experimental data, since the composite mass loss increases when the zinc volume fraction increases, describing a similar curve as the one depicted in Fig. 2 for Zn At%.

An increase in the colour histograms mean values is observed and assigned to the zinc oxide formation in the samples surfaces. Reproducibility is not as good as with not treated samples.

The dispersion between zinc amounts on each side of the composite samples was obtained in the EDX, bigger than those obtained before the acid treatment; but also on the same side, depending on the area selected to do the study, zinc amount differs considerably. That is to say that the acid attack was not homogeneous throughout the whole composite surface, due to the random formation of aggregates of zinc particles.

On the other hand, the zinc presence on the surface of the sample was drastically reduced after acid attack, while the oxygen percentage was increased. During the chemical treatment, zinc particles move to the solution as Zn^{2+} but a passivation phenomenon should be done for yielding covering layers of $Zn(OH)_2$ or ZnO, increasing that way the oxygen proportion in EDX analysis (Fig. 2). However, the decreasing loss of oxygen atoms on the surface, when the initial ratio of zinc increases after the chemical treatment, seems to indicate that the loss of mass is also due to the vinyl acetate groups.

From the values in Table 2, the overall loss of mass of each sample seems to include also polymeric material bonded to the zinc particles or/and the chemical dissolution of part of the passive layer formed. If the ratio of the C atoms on the surface remains constant after the chemical treatment and increases relatively with v_{Zn}, it is consistent with the fact that the vinyl acetate groups remains on the surface of the holes produced by the dissolution of the zinc particles. Therefore, from all the analytical results of both series of samples, before and after chemically treated, it could be said that the zinc particles much rather interact with the vinyl acetate than with the ethylene groups, but the preferred metal–metal interaction is the cause of the anomalous percolation threshold measured by the LCR bridge.

The loss of mass of zinc follows a first order kinetic described by the Eq. 3:

$$v_d = k \cdot \mathrm{At\%}_{\mathrm{Zn}} \tag{3}$$

where v_d is the zinc loss velocity, $\mathrm{At\%}_{\mathrm{Zn}}$ is the surface zinc concentration (At% value obtained in the EDX analysis for Zn), and k is the kinetic constant. It is possible to obtain k value plotting the difference of $\mathrm{At\%}_{\mathrm{Zn}}$ before and after acid treatment divided by total treatment time (34 days), that is, zinc dissolution velocity, versus $\mathrm{At\%}_{\mathrm{Zn}}$. A right line with origin in zero and $r^2 = 0.995$ was obtained; the slope is the kinetic constant: $k = 2.74 \times 10^{-2}$ days^{-1}.

Electrical properties of the bulk had been barely affected with the corrosive treatment, preserving their original order of values but with a very high dispersion of them, oscillating around the previous data as shown in Table 3. Similar observations are done from the other properties, since the loss of zinc only occurs from the surface samples. This phenomenon is more evident than the content of zinc is higher since the random distribution of the zinc particles is affected by the physical interactions between both components.

Consequently, the formation of zinc aggregates and the orientation of the polar groups to the interface polymer/metal, causes disorder with respect to an ideal composite. This behaviour should be minimized if other more accurate and sophisticated methods for preparing the sample were used. In spite of these observations the hot plate method applied on a simple mixture of the materials in powder is quick and very simple.

Conclusions

The conductance of the composite depends on the content of zinc powder, showing three different intervals: zone I for cluster formation and dielectric polarization, zone II for cluster growth (tunnelling conduction) and zone III for infinite percolation cluster formation (percolative conduction).

Optical, microscopic and electrochemical techniques indicate that the acid attack causes only the dissolution of the zinc particles placed on the surface. Then, the conductance and the bulk properties remain practically constant after acid treatment, but their dependence on zinc powder content shows more disperse results than the non-attacked samples.

Acknowledgements This work was financed by the Spanish Ministry of Science and Technology (Project ''MUVE'' MAT2000–0100-P4-03). J.J. García-Jareño acknowledges to this organism their position (''Ramón y Cajal'' Program).

References

1. Hale DK (1976) J Mater Sci 11:2105
2. Li Z, Guo S, Song W, Hou B (2003) J Mater Sci 38:1793
3. Breval E, Klimkiewicz M, Shi YT, Arakaki D, Dougherty JP (2003) J Mater Sci 38:1347
4. Al-Rawashdeh NAF, Sandrock ML, Seugling CJ, Foss CA (1998) J Phys Chem B 102:361
5. Tchmutin IA, Ponomarenko AT, Krinichnaya EP, Kozub GI, Efimov ON (2003) Carbon 41:1391
6. Psarras GC, Manolakaki E, Tsangaris GM (2003) Composites part A 34:1187
7. Oku M European Patent, Patent Application Number: 92103630.7
8. Bueche F (1972) J Appl Phys 23:2463
9. Navarro-Laboulais J, Trijueque J, García-Jarreño JJ, Vicente F (1997) J Electroanal Chem 422:91
10. Lux F (1993) J Mater Sci 28:285
11. Xen XB, Devaux J, Issi JP, Billaud D (1995) Polym Eng Sci 35:637
12. Du Pasquier A, Fáuvarque JF (1995) J Chim Phys 92:991
13. Szupkowski T (1986) Int Polym Sci Technol 13:80
14. Ruschau GR, Yoshikawa S, Newnham RE (1992) J Appl Phys 72:953
15. Song Y, Noh TW, Lee SI, Gaines JT (1986) Phys Rev B 33:904
16. Choi MS, Kim WS, Lee SI (1994) Phys Rev B 49:348
17. Navarro-Laboulais J, Trijueque J, J.J. García-Jarreño, Benito D, Vicente F (1998) J Electroanal Chem 444:173
18. Navarro-Laboulais J, Roig A, Noguera P, Vicente F, Vilaplana J, López J (1994) J Mater Sci 29:4604
19. Navarro-Laboulais J, Vilaplana J, J. López J.J. García-Jareño, Benito D, Vicente F (2000) J Electroanal Chem 484:33
20. Ahmad Z, Aleem BJA (2002) Mater Des 23:173
21. Barbosa MR, Bastos JA, J.J. García-Jareño, Vicente F (1998) Electrochim Acta 44:957
22. Dang Z, Fan L, Zhao S, Nan C (2003) Mater Res Bull 38:499
23. Rusu M, Sofian N, Rusu D (2001) Polym Test 20:409
24. Telli L, Hammouche A, Brahimi B, Doncker R (2002) J Power Sources 103:201
25. Brito Z, Sanchez G (2000) Compos Struct 48:79
26. Lide DR (1995) CRC handbook of chemistry and physics. CRC Press, New York, p 95
27. Subiela J (2006) Doctoral Thesis. University of Valencia
28. Suteerapataronon S, Jakmunee J, Vaneesorn Y, Grudpan K (2002) Talanta 58:1235
29. Sanna G, Pilo MI, Piu PC, Spano N, Tapparo A, Campus GG, Seeber R (2002) Talanta 58:979
30. Xue Q (2003) Physica B 325:195
31. Dwayner RJ, Mizes HA, Shedd G (1996) Metris-1000 scanning tunneling microscope workbook. Burleigh Instruments Inc., New York
32. Pierre C, Deltour R, Perenboom JA, Van Bentum PJM (1990) Phys Rev B 42:3380
33. Ishigure Y, Iijima S, Ito H, Ota T, Unuma H, Takahashi M, Hikichi Y (1999) J Mater Sci 34:2979
34. Balberg I (2002) Carbon 40:139
35. Xue Q (2004) Eur Polym J 40:323